AD-A097 862 AEROSPACE CORP EL SEGUNDO CA ELECTRONICS RESEARCH LAB F/G 20/5
AMPLIFICATION IN DOUBLE HETEROSTRUCTURE GAAS LASERS.(U)
MAR 81 E GARMIRE, M CHANG F04701-80-C-0081
UNCLASSIFIED TR-0081(6930-03)-2 SD-TR-81-30 NL

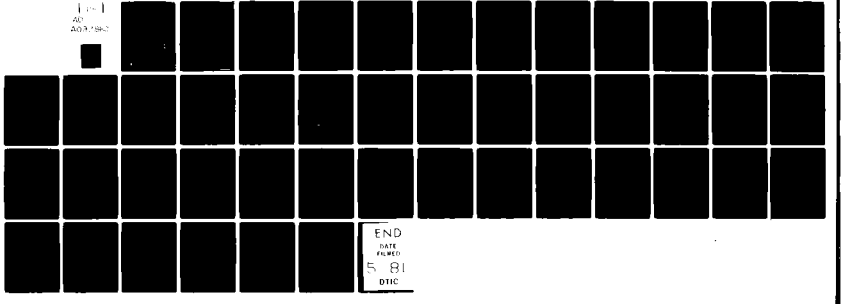

REPORT SD-TR-81-30

Amplification in Double Heterostructure GaAs Lasers

E. GARMIRE and M. CHANG, Consultant
Electronics Research Laboratory
Laboratory Operations
The Aerospace Corporation
El Segundo, Calif. 90245

15 March 1981

Interim Report

Prepared for

SPACE DIVISION
AIR FORCE SYSTEMS COMMAND
Los Angeles Air Force Station
P.O. Box 92960, Worldway Postal Center
Los Angeles, Calif. 90009

This interim report was submitted by The Aerospace Corporation, El Segundo, CA 90245, under Contract No. F04701-80-C-0081 with the Space Division, Contracts Management Office, P.O. Box 92960, Worldway Postal Center, Los Angeles, CA 90009. It was reviewed and approved for The Aerospace Corporation by M. T. Weiss, Vice President and General Manager, Laboratory Operations. Gerhard E. Aichinger was the project officer for Mission-Oriented Investigation and Experimentation (MOIE) Programs.

This report has been reviewed by the Publications Affairs Office (PAS) and is releasable to the National Technical Information Service (NTIS). At NTIS, it will be available to the general public, including foreign nations.

This technical report has been reviewed and is approved for publication. Publication of this report does not constitute Air Force approval of the report's findings or conclusions. It is published only for the exchange and stimulation of ideas.

Gerhard E. Aichinger
Project Officer

FOR THE COMMANDER

for

Evan R. Brossman, Chief
Contracts Management Office

UNCLASSIFIED

SECURITY CLASSIFICATION OF THIS PAGE *(When Data Entered)*

19 REPORT DOCUMENTATION PAGE	READ INSTRUCTIONS BEFORE COMPLETING FORM
1. REPORT NUMBER (18) SD-TR-81-30 / 2. GOVT ACCESSION NO. AD A097862	3. RECIPIENT'S CATALOG NUMBER
4. TITLE *(and Subtitle)* (6) AMPLIFICATION IN DOUBLE HETEROSTRUCTURE GaAs LASERS.	5. TYPE OF REPORT & PERIOD COVERED (9) Interim rept.
	6. PERFORMING ORG. REPORT NUMBER (14) TR-0081(6930-03)-2
7. AUTHOR(s) (10) Elsa Garmire and Michael Chang, Consultant	8. CONTRACT OR GRANT NUMBER(s) (15) F04701-80-C-0081
9. PERFORMING ORGANIZATION NAME AND ADDRESS The Aerospace Corporation El Segundo, Calif. 90245	10. PROGRAM ELEMENT, PROJECT, TASK AREA & WORK UNIT NUMBERS
11. CONTROLLING OFFICE NAME AND ADDRESS (11) Space Division Air Force Systems Command Los Angeles, Calif. 90009	12. REPORT DATE 15 March 1981
	13. NUMBER OF PAGES 45
14. MONITORING AGENCY NAME & ADDRESS *(if different from Controlling Office)* (12) 46	15. SECURITY CLASS. *(of this report)* Unclassified
	15a. DECLASSIFICATION/DOWNGRADING SCHEDULE

16. DISTRIBUTION STATEMENT *(of this Report)*

Approved for public release; distribution unlimited

17. DISTRIBUTION STATEMENT *(of the abstract entered in Block 20, if different from Report)*

18. SUPPLEMENTARY NOTES

19. KEY WORDS *(Continue on reverse side if necessary and identify by block number)*

Amplifier
GaAs
Integrated Optics
Regenerative Amplifier

20. ABSTRACT *(Continue on reverse side if necessary and identify by block number)*

Regenerative amplification has been measured in a DH GaAs laser in two different geometries, including both discrete and integrated optics configurations. Regimes of strong and weak signal gains have been identified and measured, with gains being as large as 170. Comparison has been made between the experimental results and theoretical models. In general, the agreement is excellent. Details of the experiments and theoretical models are presented in this report.

DD FORM (FACSIMILE) 1473

392106

SECURITY CLASSIFICATION OF THIS PAGE *(When Data Entered)*

CONTENTS

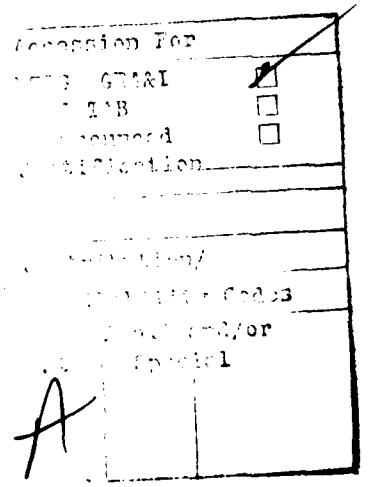

FIGURES

Introduction

Measurements were made of regenerative amplification in two configurations: a close-coupled oscillator/amplifier configuration and a weak-coupled configuration. The close-coupled configuration consisted of a laser and amplifier region on the same substrate, the regions being defined by a cleave in the laser chip. The weak-coupled configuration consisted of a laser whose output is reflected back into an amplifying portion of the same device. In each of these cases, qualitative agreement could be made with laser amplifier theory in the strong signal and weak signal cases, when regeneration is included. The largest value of gain measured in these experiments was 170.

Practical uses of laser amplifiers will most likely be in neither the strong signal regime nor the weak signal regime, but in an intermediate regime where gains are the largest. In this intermediate regime, it is necessary to take into account both regeneration and saturation of the gain. It is proposed to continue the theoretical and experimental studies to include this regime.

An important consideration is the high frequency response of the amplifier. Preliminary measurements were inhibited by capacitance effects and cross-talk between the laser and amplifier. Fast-response can be deduced, however, from the fact that when pulsed, ripples in the optical output were reproduced by the amplifier at speeds up to our detection limit of 10 nsec. It is proposed in the next part of the study to purposely modulate the laser and measure the amplification as a function of modulation speed.

Theory of Travelling Wave Amplifiers

The theoretical approach we follow is to consider first the travelling wave amplifier, and then add regeneration by considering multiple reflections from the mirrors.

The theory of the travelling wave amplifier is based on the rate equations for the conservation of electrical carriers and light intensity. Changes in the light intensity are caused by the emission or absorption of light, while the changes in the carrier density are due to carrier injection, spontaneous emission, and stimulated emission or absorption. These mechanisms lead to the following equations:

$$\frac{\partial I}{\partial z} + \frac{1}{v} \cdot \frac{\partial I}{\partial t} = g(N) I \tag{1}$$

$$\frac{\partial N}{\partial t} = S - \frac{N}{\tau} - g(N) I \tag{2}$$

where I is the light intensity in the mode of interest, v is the velocity of light in the medium, N is the population density of excited carriers, τ is their relaxation time, and S is the injection rate. The gain (or absorption) depends, in general, on the number of carriers present in the active layer. The exact form will depend on the model assumed for the laser. Finally, the injection rate is related to the injected current density, J, by

$$S = J \eta / ed \tag{4}$$

where η is the internal quantum efficiency, e is the electronic charge, and d is the active layer thickness.

A steady state analysis is used to simplify equations (1) and (2). This assumption is valid for DC amplification or for pulsed amplification when the pulse length is much

longer than the relaxation time of the carriers (~1ns). Assuming steady state, equations (1) and (2) respectively become

$$\frac{\partial I}{\partial z} = g(N)\, I \tag{5}$$

$$\frac{N}{\tau} = S - g(N)\, I. \tag{6}$$

These two equations are coupled through the dependence of the gain, g, on the carrier density, N. Without making specific assumptions as to the form of the gain, these two equations can be combined into a single non-linear differential equation, which can be solved for specific models of the dependence of gain on the carrier density. Equation 6 can be rewritten as

$$I = \frac{S - N/\tau}{g(N)} ,$$

differentiated with respect to z, and inserted into the left hand side of equation 5. The following general non-linear differential equation is obtained:

$$\frac{N}{z}\left\{ g(N)/\tau + \frac{\partial g(N)}{\partial N} \cdot (S - N/\tau) \right\} + g^2(N)(S - N/\tau) = 0 \quad . \tag{7}$$

Let us now make specific assumptions as to the form of g (N). The simplest model of the GaAs laser is a two-level model in which the valence and conduction bands represent the two levels. In this model there is no saturation, and

$$g = g_o \left(\frac{N}{N_s} - 1 \right),$$

where N_s is the carrier density at which the material becomes transparent. A more accurate model of the semiconducter laser, however, includes the fact that the bands are broad and are described by densities of state. This means that gain occurs most strongly

for carriers nearest the bandedge. This means that relaxation of carriers from deeper in the band to the band edge must be included in the laser model. This relaxation will have a characteristic time and will result in saturation of the number of possible carriers in the excited state. This is expressed in a heuristic fashion by writing

$$g(N) = g_o \frac{\left(\frac{N}{Ns} - 1\right)}{\left(1 + \frac{N}{Ns}\right)} \tag{8}$$

where N_s is the saturation density (the number of carriers required to equalize the population densities in the upper and lower states). The weak signal absorption coefficient, g_o, and the parameter γ are quantities determined from absorption measurements.

Using this form for the gain, we can rewrite equation 7 as

$$\frac{\partial N}{\partial z} \cdot (a - 2bN_sN - bN^2) + g_o (N-N_s)^2 (S-N/\tau) = 0 \tag{9}$$

where $a = S(1+\gamma)N_s + N_s^2/\tau$ and $b = \gamma/\tau$. In principle, this equation can be integrated, the proper boundary conditions applied, and the behavior of a travelling wave amplifier can be determined. For the purpose of this report we shall consider analytic solutions under two conditions, the large signal and small signal limits. The intermediate regime will be the subject of next year's work.

Two simple cases in which the amplifier behavior can be derived analytically are cases in which the gain in the amplifier is a constant. This occurs when the carrier density is independent of position. In such cases, referring to equation 7, either the gain coefficient, g, is zero, or $S = N/\tau$. These two cases correspond to the large and small signal limits respectively. Referring to equation (6), the small signal limit implies that $S \gg g(N) I$. This means that the injection rate of carriers is much larger than the change in carrier density due to absorption or emission. Hence, the incident light is

small. This small signal regime will be discussed first. The other case in which the amplifier is transparent is when $g(N) = 0$. For the form of the gain assumed here, this means that $N = N_s$. In this strong signal regime, the number of carriers in the upper and lower states are equal. The large signal means that the increase in the number of carriers due to current injection is insignificant compared to the changes caused by the absorption and emission of light. Since the rate of absorption and emission will be equal, the gain coefficient is zero. This large signal regime will be discussed second.

In these two regimes gain is independent of position and regeneration can be included easily. The theory of regenerative amplifiers will be included in the next section.

The small signal limit corresponds to the case in which the rate of change of carriers is dominated by the injection rate so that the change due to stimulated emission can be neglected. In this case gI is much less than S and equation (6) becomes $N = S\tau$. From equation (5), with g (N) equal to a constant $g(S\tau)$, the intensity is given by

$$\ln \quad (I/I_o) \quad = \quad g\,(S\,\tau) \quad z \quad . \tag{10}$$

The intensity grows exponentially with distance.

For the saturable two-level laser model, with a gain given by equation (8), the intensity of an amplifier of length L is determined by

$$\ln\ (I/I_o) \quad = \quad g_o L \quad \frac{S\tau - N_s}{\gamma S\tau + N_s} \quad . \tag{11}$$

Since S is dependent on current, it can be seen that the intensity coming out a fixed length amplifier grows exponentially with current until saturation is reached, at which point the gain tends to a constant value given by $g_o L/\gamma$.

The other limit which can be solved analytically is the large signal limit, where $N = N_s$ and the two levels are driven to have equal populations. In this case, equations 6 and 5 can be combined to yield

$$\frac{\partial I}{\partial z} = S - N_s/\tau.$$

Direct integration gives a linear growth with length:

$$I = (S - N_s/\tau)\, z + I_o. \tag{12}$$

It can be seen that in the large signal limit, for an amplifier with a fixed length, the light out is equal to the light in plus an additional contribution which is linearly proportional to current. To compare experiment with theory in the large signal limit, it will be of interest to look at the difference between the input and output signals rather than the ratio of incident to output signals, which was the relevant parameter in the small signal limit. If the gain is defined as the ratio of the output to the input signals, it can be written as:

$$G = I/I_o = (S-N_s/\tau)L/I_o + 1 \tag{13}$$

In the limit of a very large input signal, the gain is one and there is no amplification. The amplifier is transparent. Measurements of amplification in the double heterostructure lasers will be compared to each of these two limits.

Theory of Regnerative Amplifiers

In order to consider the effects of regeneration, in an exact model, one must generalize the conservation equations and use Maxwell's equations with a non-linear polarizability, which expresses the relationship between the carriers and the electromagnetic field, rather than the intensity. One then gets a non-linear electromagnetic

wave equation. However, this equation is easily solvable only in cases where the gain is constant over the length of the amplifier. When this is the case, the regenerative amplifier can also be calculated by considering successive bounces of a travelling wave. This has been done, for example, in the book by Siegman.

When the laser signal which is to be amplified is a single mode, it is important to include the possibility that the resonance frequency of the amplifier does not match the laser frequency. This leads to an equation for the transmitted intensity I in terms of the incident intensity I_o given by

$$\frac{I}{I_o} = \frac{T_1 \; T_2 \; G}{(1 - RG)^2 \; + \; 4 \, GR \sin^2 (k_o nL)} \tag{14}$$

where $k_o = \frac{2\pi}{\lambda_o} = \frac{2\pi\nu}{c}$ and ν is the laser frequency.

L is the distance between amplifier mirrors, $T_1 = 1 - R_1$, $T_2 = 1 - R_2$, where R_1 and R_2 are the reflectivities of the two mirrors of the regenerative amplifier, not necessarity equal; $R^2 = R_1 R_2$ and G is the single pass gain of the amplifier.

When the incident light signal is not monochromatic, this expression must be integrated over the frequency dependence of the incident signal. In particular, the transmitted signal will be given by

$$I_T = \frac{1}{2\Delta\nu} \int_{-\infty}^{\infty} \frac{T_1 \; T_2 \; G}{(1 - RG)^2 \; + \; 4GR \sin^2 \left(\frac{2\pi\nu nL}{c}\right)} \; I_o(\nu) \, d\nu . \tag{15}$$

This assumes that the detector integrates over a bandwith $\Delta\nu$ which is much larger than the spectrum of the laser input. In general, G is a function of frequency through its dependence on I_o.

In the cracked-substrate experiments, the laser signal could not be resolved into individual modes, even with narrow slits in the monochromator. This is presumably due

to the fact of heating in the junction during the laser pulse. As a result, the laser signal was broader than the resonances of the amplifier, and it is necessary to perform the integration of equation 15. For this purpose it is sufficient to assume that the laser signal is constant over its linewidth and zero elsewhere. The gain is considered to be independent of frequency within the laser linewidth, and the integration is taken over several amplifier resonance periods. This leads to the following expressions for the transmission of the regenerative amplifier, depending on whether the amplifier is in the weak or strong signal regime. The results are: Small signal limit:

$$I = I_o \frac{T_1 T_2 e^{g L}}{1 - R_1 R_2 e^{2 g L}} \tag{16}$$

Large signal limit:

$$I = I_o (1 - R)/(1 + R) + \frac{1 + R^2}{(1 + R)^2} \left\{ SL - \frac{NL}{\tau} \right\} \tag{17}$$

where

$$R = \sqrt{R_1 R_2}$$

$$S = J \eta / ed$$

$$g = g(S \tau) \approx (S \tau / N_s) g_o.$$

The difference between the travelling wave amplifier and the regenerative amplifier in the small signal limit (when the gain coefficient, g, is small) is a factor, $T_1 T_2$. However, when the gain coefficient is not small and the amplifier approaches resonance (the lasing threshold), the regenerative amplifier output rises much faster with input intensity than the exponential curve of the travelling wave model.

In the strong signal regime, the functional form of the amplifier intensity is the same for both the travelling wave model and the regenerative amplifier model. Both are

linear with the injected current and the amplifier length. However, the regenerative amplifier equation has an additional factor due to reflectances off the amplifier ends. For a GaAs diode, this factor is 1.8.

The intensity out of the amplifier for a small injection rate, S, in the small signal limit, is exponential with length and current. However, as the injection rate, S, becomes larger, regeneration becomes more important. From the form of equation 16, we can determine how close to threshold one can operate before the affects of regeneration become important. Assuming the gain is a linear function of current,

$$g = g_{th} \frac{(J - J_{th})}{J_{th}} + g_{th}. \tag{18}$$

At threshold,

$$g_{th}L = -\ln R \tag{19}$$

The conditions for requiring the inclusion of regeneration are that $R\exp gL \rightarrow 1$. Using (18), this becomes $R\exp(g_{th}L(J - J_{th})/J_{th})\exp(g_{th}L) \rightarrow 1$. From (19), we have $\exp(g_{th}L(J-J_{th})/J_{th}) \rightarrow 1$. This condition reduces to $g_{th}L(J - J_{th})/J_{th} \rightarrow 1$ or to $((J - J_{th})/J_{th})(-\ln R) \rightarrow 1$. In other words, only when the amplifier current is near its threshold value, must regeneration be included.

Cracked Substrate Lasers

The cracked substrate laser is a laser closely coupled to an amplifier, fabricated by the cracked-substrate technique, described below. The device geometry is shown in Fig. 1a. This technique has the advantage of not requiring careful alignment between separate lasers and amplifiers, and makes it possible to obtain results conveniently. Later experiments will include a third region between the laser and amplifier, Fig. 1b.

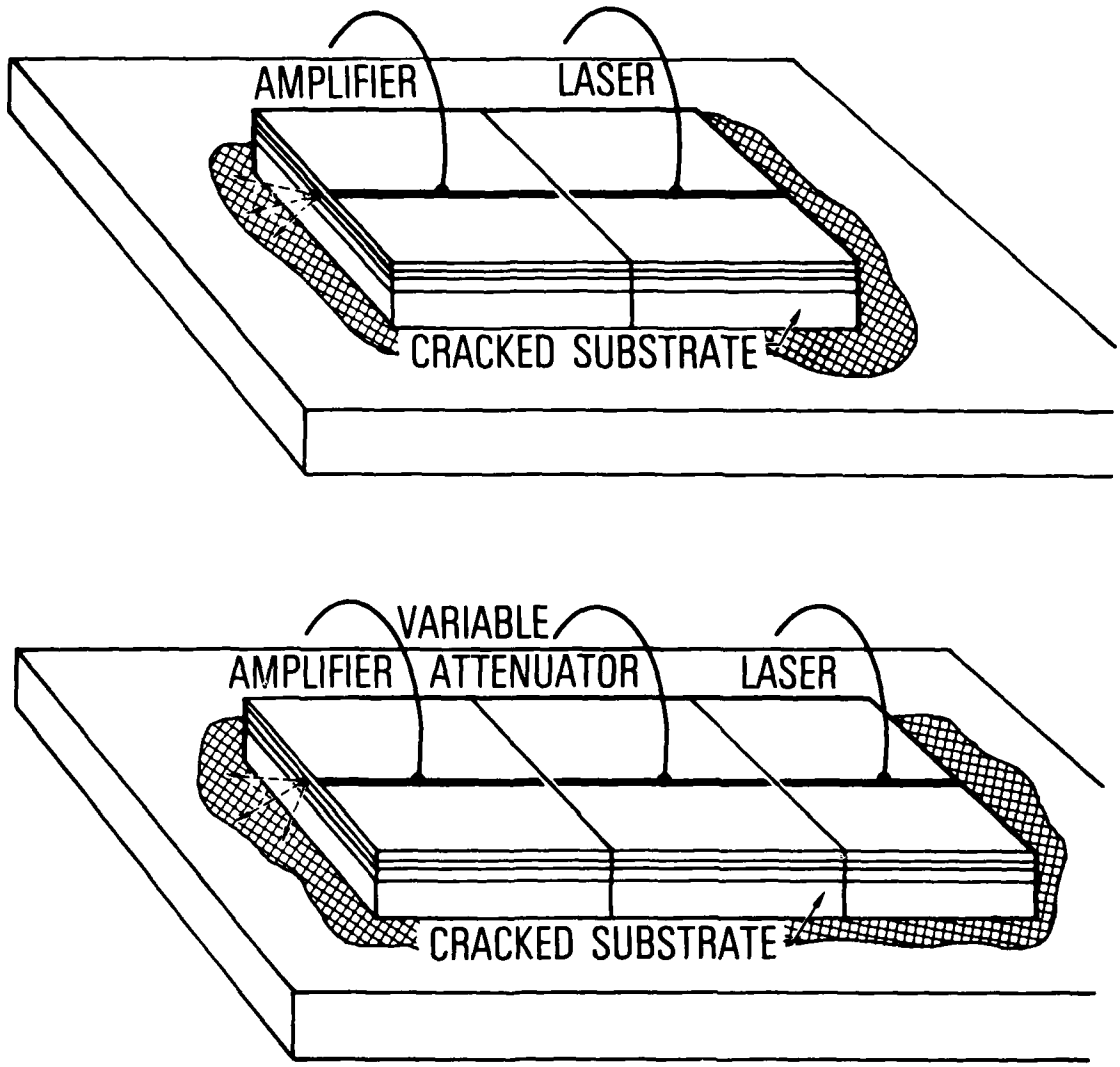

Fig. 1 Geometry of cracked substrate lasers. The chip is mounted with indium solder on a flexible gold plate and a cleave is introduced to separate the laser and amplifier regions. In Fig. 1b, a third region is introduced, which acts as a variable attenuator.

By applying a current to this intermediate region to change it from an absorbing region to transparent region, the coupling between the laser and amplifier can be varied. This device is also a model for the integrated DBR laser-amplifier structures which will be measured later in the contract.

The cracked substrate introduces a reflective plane into an integrated optics circuit and makes it possible for one region of a GaAs heterostructure wafer to be used as a laser while the remaining portion can be used for the functions. In this work we use devices which have only a laser and amplifier regions. The continuation of the effort will include a central absorbing (or transparent) region which will allow us to vary the coupling between the amplifier and the laser.

The cracked substrate devices are made by mounting a cleaved laser diode, which is twice as long and three times as wide as the usual geometry to produce single lasers. These diodes have stripe geometry contacts formed by pulse plating techniques. These large diodes are mounted by Indium solder onto a flexible, gold coated plate, typically 5 mm x 5 mm. A diamond scribe is used to create a nick at the position where a cleave is desired. The plate is then bent slightly and a cleave propagates from the nick. The yield of this process is typically 50%. The reason for using diodes which are wide is to ensure that a good quality cleavage plane develops; it has been found that it takes a few hundred microns of propagation before the crack becomes a good cleavage plane. These gold covered plates are mounted to TO5 cans and bonded in the usual fashion.

The amplification was measured by monitoring the signal out the amplifier region as a function of current applied to either the laser or amplifier segments. The light was monitored through a monochromator to ensure that only the laser light was observed and to eliminate spurious spontaneous emission from the amplifier.

Typical data are shown in Fig. 2. The light out the amplifying region was measured while keeping the amplifier voltage constant and varying the laser voltage. The increase in signal for an applied amplifier voltage represents the amplification of the device. Device L7C20 operated in the strong signal limit, as demonstrated by plotting the light out on a linear plot as a function of amplifier voltage (current); this is shown in Fig. 3. It can be seen that the light out is a linear function of amplifier voltage, and that the intercept is a linear function of laser voltage (and presumably of incident light intensity). This is in excellent qualititative agreement with the theoretical equation 17. We shall now use the theory to obtain approximate numbers for the laser parameters to demonstrate numerical agreement between experiment and theory.

Note from equations (4) and (17) that

$$\partial I/\partial J = \eta L \left\{ \frac{1 + R^2}{1 - R^2} \right\} / ed \quad . \tag{20}$$

It was necessary experimentally to calibrate the photodetector so that $\partial I/\partial J$ could be expressed in the proper units. Measurements were made on the laser amplifier through a monochromator with a photomultiplier. Calibration of this detector was made by comparing this signal to that of a photodiode, which was in turn calibrated with an energy meter using a cw Krypton laser source at 7880Å. The experimentally determined calibration was that 1 mW of power corresponded to 60 mV signal on the photomultiplier. This means that power P could be expressed as V_{PM}, voltage monitored on the photomultiplier, by the expression

$$P = CV_{PM} \tag{21}$$

where C = 0.017 mW/mV.

The light power is related to the intensity, in photons per cm^2 per second, by the expression

$$I = P/wdh\nu \, , \tag{22}$$

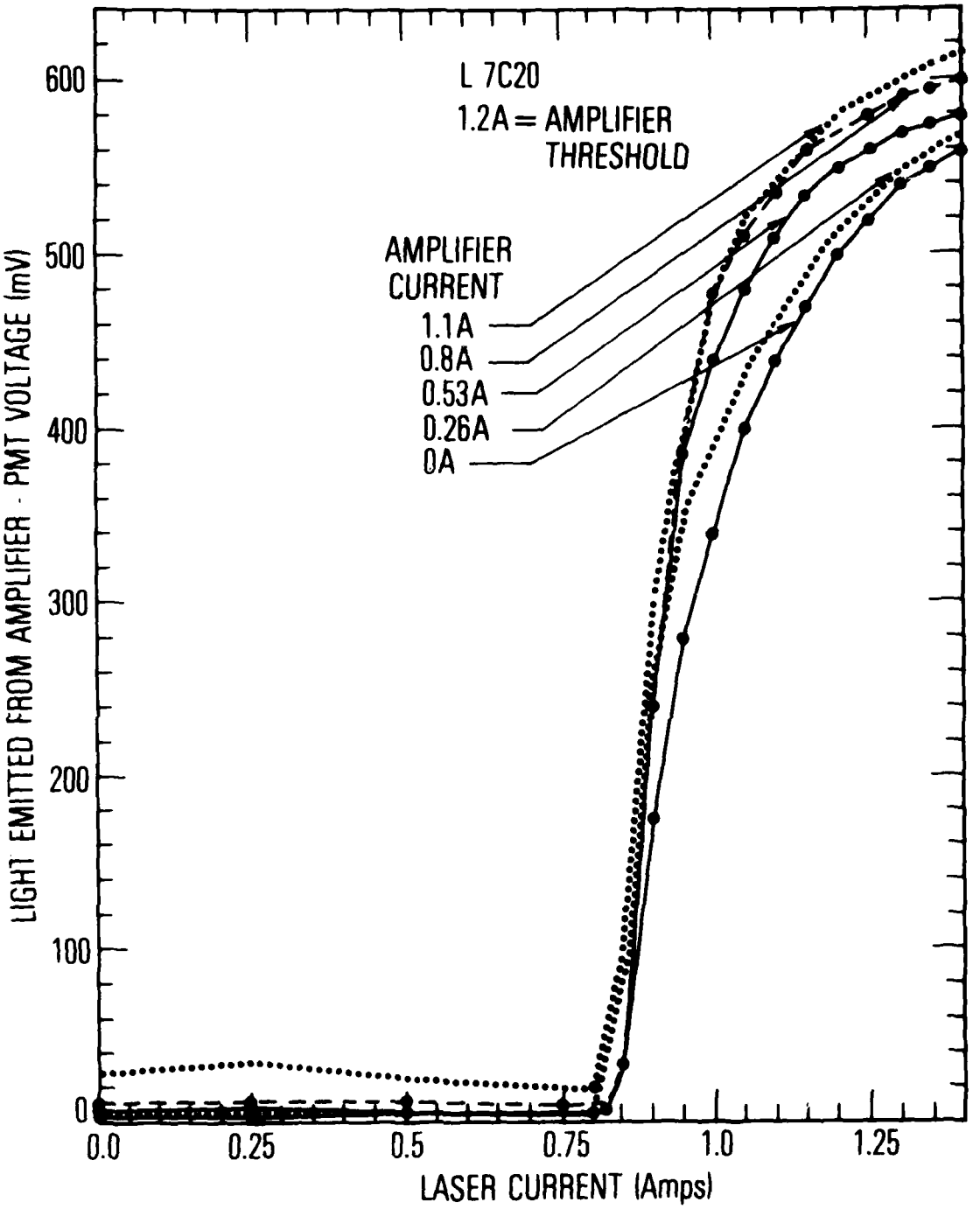

Fig. 2 Light emitted from the amplifier portion of the cracked substrate device as a function of current applied to the laser portion of the chip. Data for various amplifier currents are shown.

where w is the width of the laser stripe and d is the thickness of the active laser layer. The current density is related to the total current in amps, A, by

$$J = A/wL \tag{23}$$

where L is the length of the laser. Combining these three equations with equation 20, one obtains the equation which can be compared to the experimental curves:

$$\frac{dV_{PM}}{dA} = \frac{\eta h \nu}{Ce} \left(\frac{1 - R^2}{1 + R^2}\right). \tag{24}$$

Inserting the appropriate numbers, ($R^2 = 0.1$), and assuming $\eta = 0.5$ (appendix I), the theoretical estimate for the slope of the photomultiplier signal with amplifier current is

$$\frac{dV_{PM}}{dA} = 34. \tag{23}$$

The experimental slope, determined from Fig. 3, is

$$\frac{dV_{PM}}{dA} = 52.$$

Given the uncertainty of the calibration of the photomultiplier, we consider this excellent agreement.

We see experiment and theory agree for the slope shown in Fig. 3. It can also be seen that when the incident laser power is reduced, the theory is no longer completely valid and the slope changes. That is, the large signal limit no longer applies. The intercept gives information as to the absorption of the device, if the incident light level is known. The intercept is a measured point; the light level measured with the amplifier turned off. This is equal to the incident light level minus the saturated absorption:

$$I_c = I_o \left(\frac{1 - R}{1 + R}\right) - (N_s/\tau) \left(\frac{1 + R^2}{(1 + R)^2}\right) L \tag{24}$$

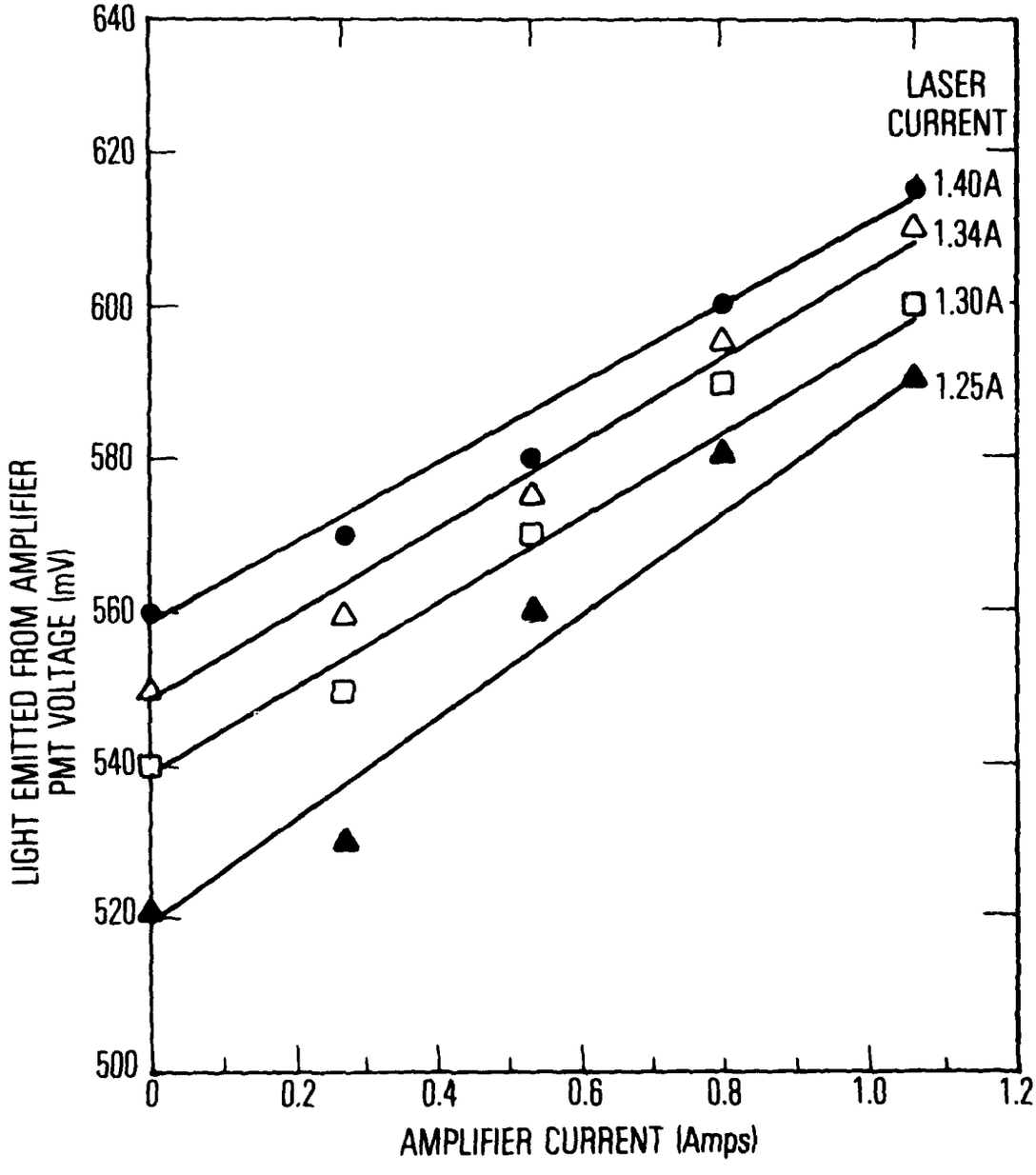

Fig. 3 Light emitted from the amplifier portion of the cracked substrate device as a function of amplifier current. Data for various laser currents are shown. This device is L7C20.

We are not able to get useful information out of this because we were not able to make a separate measurement of I_o. Although we could measure the light intensity coming out the other end of the laser, we did not know what the incident intensity was at the crack interface, and so we did not know what fraction of that intensity was coupled into the laser. The fact that the intercepts are equally spaced as a function of laser voltage is due to the fact that at these operating voltages, the laser intensity is indeed a linear function of voltage. This can be seen in Fig. 3, with the amplifier off.

It can be seen that the actual gain in the large signal regime is very small. The measured gain was roughly 1.1. Clearly the amplifier used under such a situation is an excellent optical limiter, but a poor amplifier. The small signal limit in this device occurred right at laser threshold and was very difficult to measure since it was swamped by fluctuations in the laser output.

We were able to use the cracked substrate geometry to look at small gains by observing the frequency dependence of the gain. We chose a device which had different oscillation frequencies in the laser and amplification portions, measured when each was separately excited.

It can be seen from equation 6 that the strong signal regime occurs when gI is much larger than S. To leave this limit and go into the regime where $gI \ll S$, one can either decrease the light intensity or decrease the gain. By using a laser signal incident on an amplifier whose peak amplification is at a different wavelength, g can be made small enough that the weak signal limit is valid. We did, indeed, observe the exponential gain with current predicted by equation (11) for small signals.

Data was taken at a fixed laser current, above threshold. The amplifier output was measured as a function of amplifier current at both the wavelength of the peak

amplifier gain and at the wavelength of the laser frequency. The data is shown in Fig. 4. The weak signal case is at 8729Å, and the strong signal case is at 8768Å, at which frequency the amplifier could oscillate. The weak signal data has been fit by two curves, shown in Fig. 5. The solid curve is the regenerative amplifier fit from equation 16, while the dotted curve is the exponential fit of the travelling wave amplifier (equation 11). The better fit by the regenerative amplifier model is easily seen. From this fit, the small signal absorption coefficient of the unpumped amplifier, $\alpha_o = -g_o$, can be determined to be 14 cm^{-1}. This value is comparable to those published* and indicates that we have good agreement between experiment and theory for the regenerative amplifier in the small signal limit.

Further comparison between experiments and theory can be made by considering the order of magnitude of the saturation density, N_s. From the fit to equation 14,

$$gL = 1.14\, i, \tag{25}$$

where i is the applied amplifier current. Using equation 8 in the small signal limit

$$1.14 = \frac{\alpha_o \eta \tau}{edwN_s} . \tag{26}$$

For $d \approx 0.26\ \mu m$, $w = 47\ \mu m$, $\eta = 0.5$

$$\frac{N_s}{\tau} = 3 \times 10^{26}\ cm^{-3}\, sec^{-1}. \tag{27}$$

For a relaxation time, $\tau =$ 1ns, the saturation density is

$$N_s \sim 10^{17}\ cm^{-3}. \tag{28}$$

*Thompson, etal. JAP 27 (4) p.1501 (April 1976)

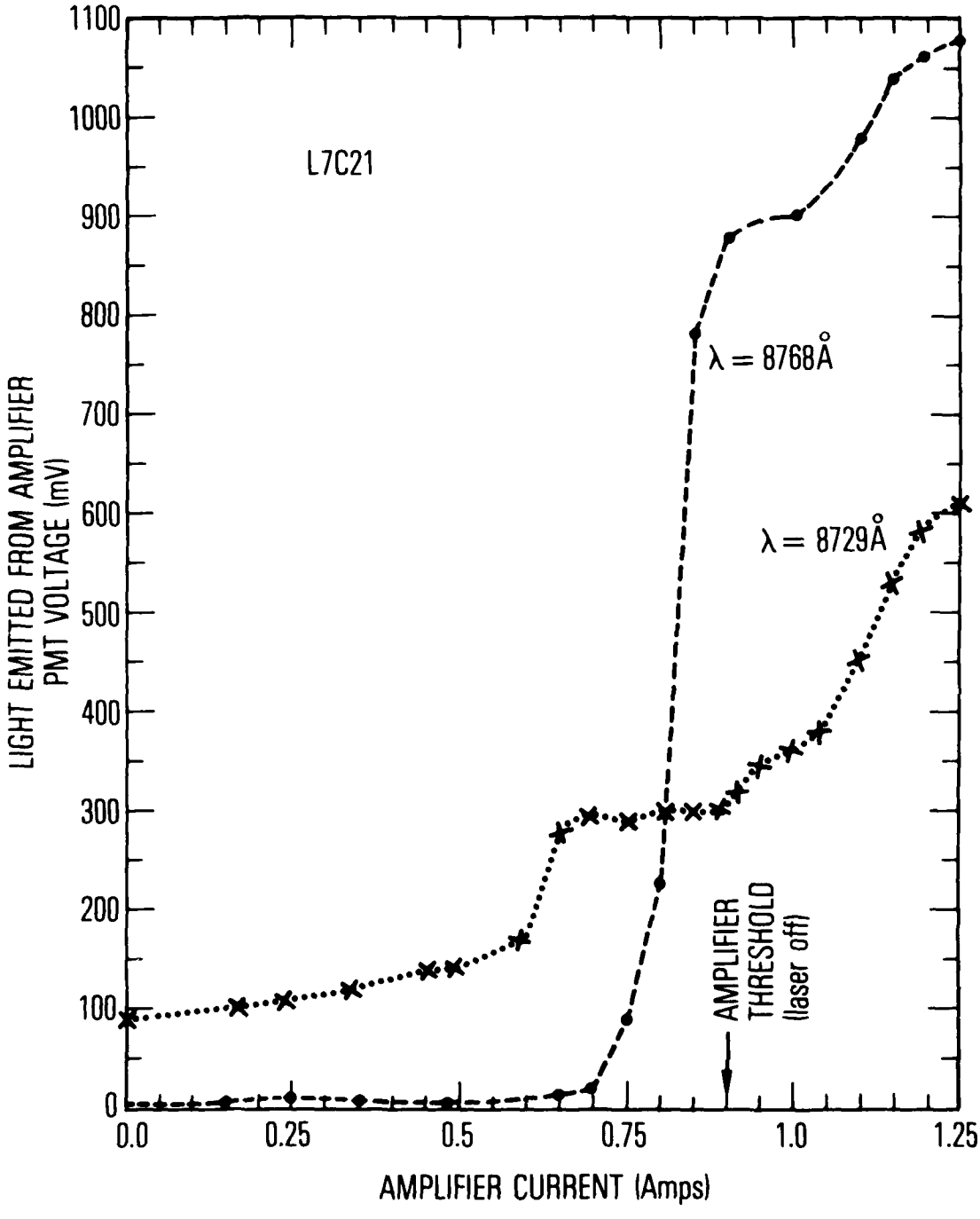

Fig. 4 Light emitted from the amplifier region of device L7C21 as a function of amplifier current, for a fixed laser current. The signal was measured through a monochromator set at two different frequencies.

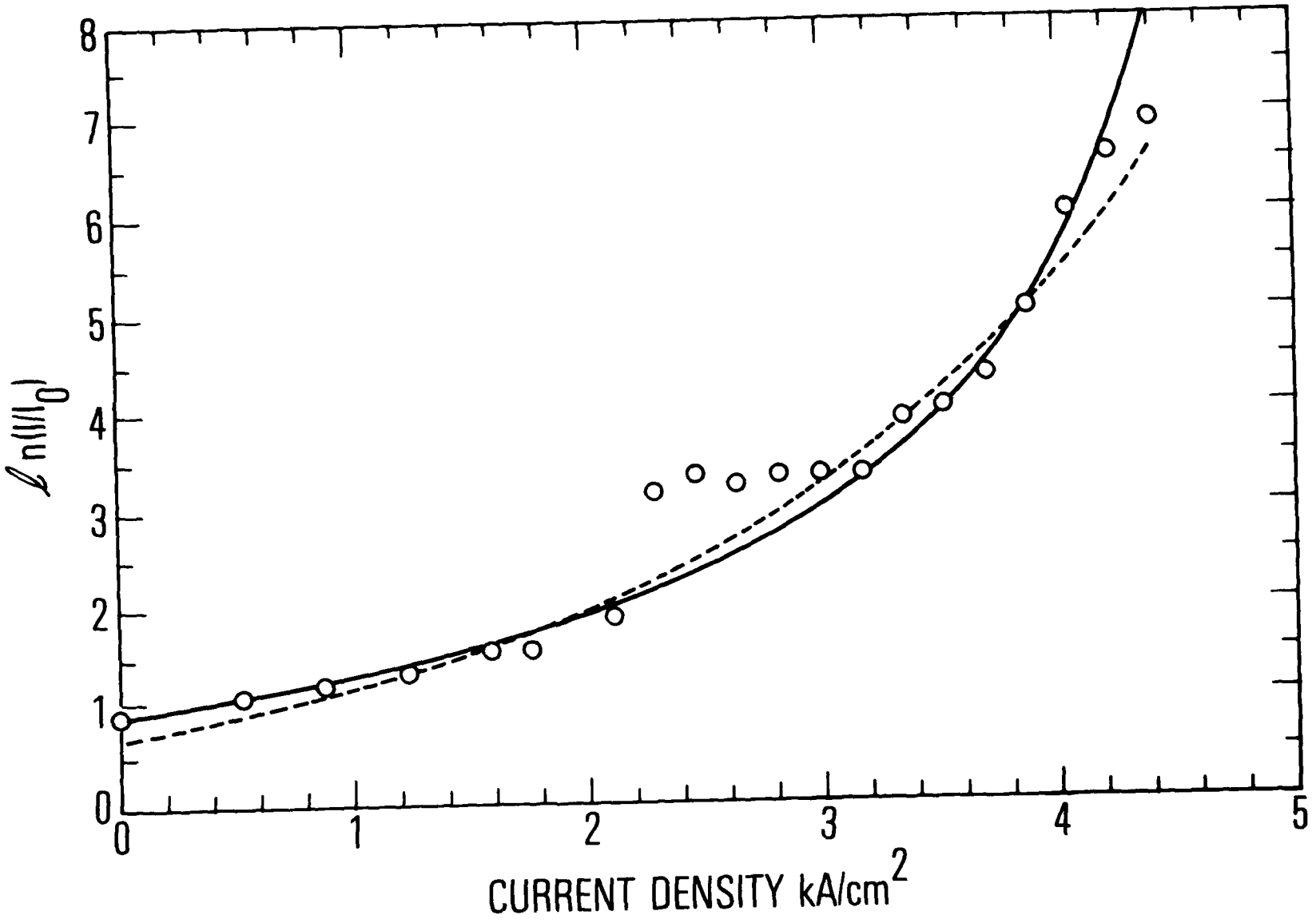

Fig. 5 Measurements and theoretical models for the weak signal amplifications observed at 8729 Å. The dotted line corresponds to the traveling wave analysis and the solid line to the regenerative amplifier theory.

This density is comparable to the doping density of the active layer and lends confidence to our interpretation.

An additional comparison between the experimental curve and the theoretically predicted curve can be made in terms of the amplifier threshold. In the small signal limit, the gain is

$$g = g_o \left(\frac{S}{N_s} - 1\right). \tag{29}$$

When no current is injected ($S = 0$), the gain is negative and the amplifier is absorbing. The gain is

$$g\,(S = 0) = -g_o. \tag{30}$$

As the injected current is increased, the gain (or absorption) goes to zero and the amplifier becomes transparent. When the amplifier is transparent, the injection rate is

$$S_o = N_s/\tau. \tag{31}$$

Combining equations 29, 30, and 31

$$g = \left(\frac{S}{S_o} - 1\right). \tag{32}$$

Because the injection rate is proportional to the injected current, the gain can be written

$$g = \left(\frac{J}{Jo} - 1\right). \tag{33}$$

With the experimental setup, the current at which the amplifier becomes transparent, J_o can not be determined since there was no way to monitor the light incident to the amplifier. However, the current resulting in transparency can be related to the current at the lasing threshold. The lasing threshold occurs when

$$g_{th} L = - \ln R. \tag{34}$$

Substituting this equation into equation 24, J_o can be related to J_{th}:

$$Jo = \frac{J_{th}}{1 - \frac{\ln R}{\alpha L}} \tag{35}$$

Rewriting the gain in terms of the threshold current,

$$gL = \frac{J}{J_{th}} (2L - \ln R) - \alpha L. \tag{36}$$

Using a measured value for the threshold current this equation can be compared with theory. For $\alpha = 14\ cm^{-1}$, L = 0.043 cm, R = 0.32, and a threshold current of 1.1 amps, we obtain

$$gL = 1.5\ i - 0.60$$

where i is the applied amplifier current. The coefficient for the amplifier current, 1.5, is in good agreement with the experimentally measured value of 1.14. Again we have demonstrated that the small signal regime is understood theoretically.

Since the signal from a regenative amplifier can be large even in the absence of laser input, it is important to define the gain properly. Amplifier gain is determined from the signal of the amplified laser minus the signal from the amplifier with the laser off (to eliminate any amplified spontaneous emission in the amplifier) normalized to the incident laser signal. Plots of this are shown in Fig. 6. This data shows the proper exponential dependence on current and agrees with theory for currents below the lasing threshold. The peak gain, at just below threshold, is about five.

This presentation of the data enhances the anomaly around 1.2 V. At this current, the amplifier gain at 8729Å starts to become super-linear. However, at a slightly larger current, another frequency with a larger gain, 8768Å, begins to lase and, in the competition for carriers, quenches the oscillation at 8729Å. It is only at larger currents, when the gain at 8768Å saturates, that the line at 8729Å begins to lase.

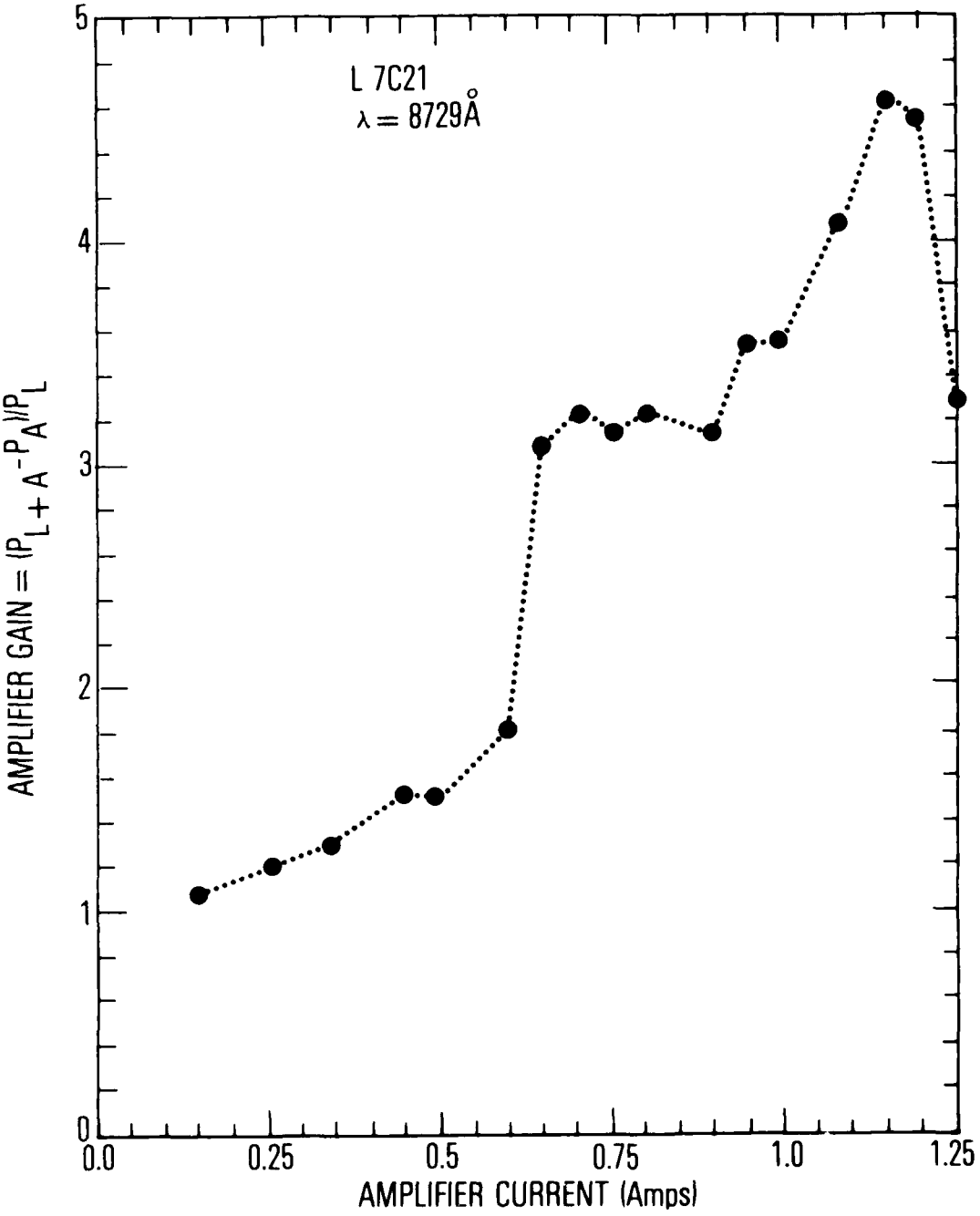

Fig. 6 True amplifier gain: Signal with current applied to both the laser and amplifier regions minus the signal with current applied only to the amplifier, divided by the signal with current applied only to the laser. This is the weak signal case at 8729Å.

The data at 8768Å shown in Fig. 4 are better fit by a coupled oscillator model than by the theory of regenerative amplification. Regeneration plays a dominant role in this device, since it can be observed that the amplifier begins to lase. In fact, the threshold of the amplifier is lowered by the presence of the laser light. It is in this oscillation regime that high gains are observed. The amplifier gain is defined as

$$G = \frac{P_{AL} - P_A}{P_L}$$

where P_{AL} is the signal measured with both the laser and amplifier operating, P_A is the signal coming from the amplifier in the absence of any incident laser signal, and P_L is the signal coming from the laser, as measured through the amplifier with no signal applied to the amplifier. The measured data is shown in Fig. 7. It can be seen that the gain is very large at a particular operating region, just below oscillation threshold for the amplifier (0.9 amps in the absence of laser input). The presence of laser light appears to cause the amplifier to oscillate at the lower current of 0.75 amps and the gain gets very large. This is the regime that needs more study to obtain information as to the high speed frequency response of this region, as well as its ability to maintain the phase of a signal. But whether this is true oscillation or very large amplification remains subject for study. In this mode of operation it can be seen that the gain can reach 170. More experiments are underway.

Comparison with theory requires the study of coupled oscillators a model in which the amplifier is above oscillation threshold. The way in which the two oscillators are coupled can be seen from plotting the threshold for oscillation of the coupled laser-amplifier system as a function of the laser current and the amplifier current. This is shown in Fig. 8. It can be seen that the presence of some current in the amplifier has a slight affect on the laser threshold, decreasing it somewhat. However, it can be seen that the presence of current in the laser region has a strong affect on the amplifier

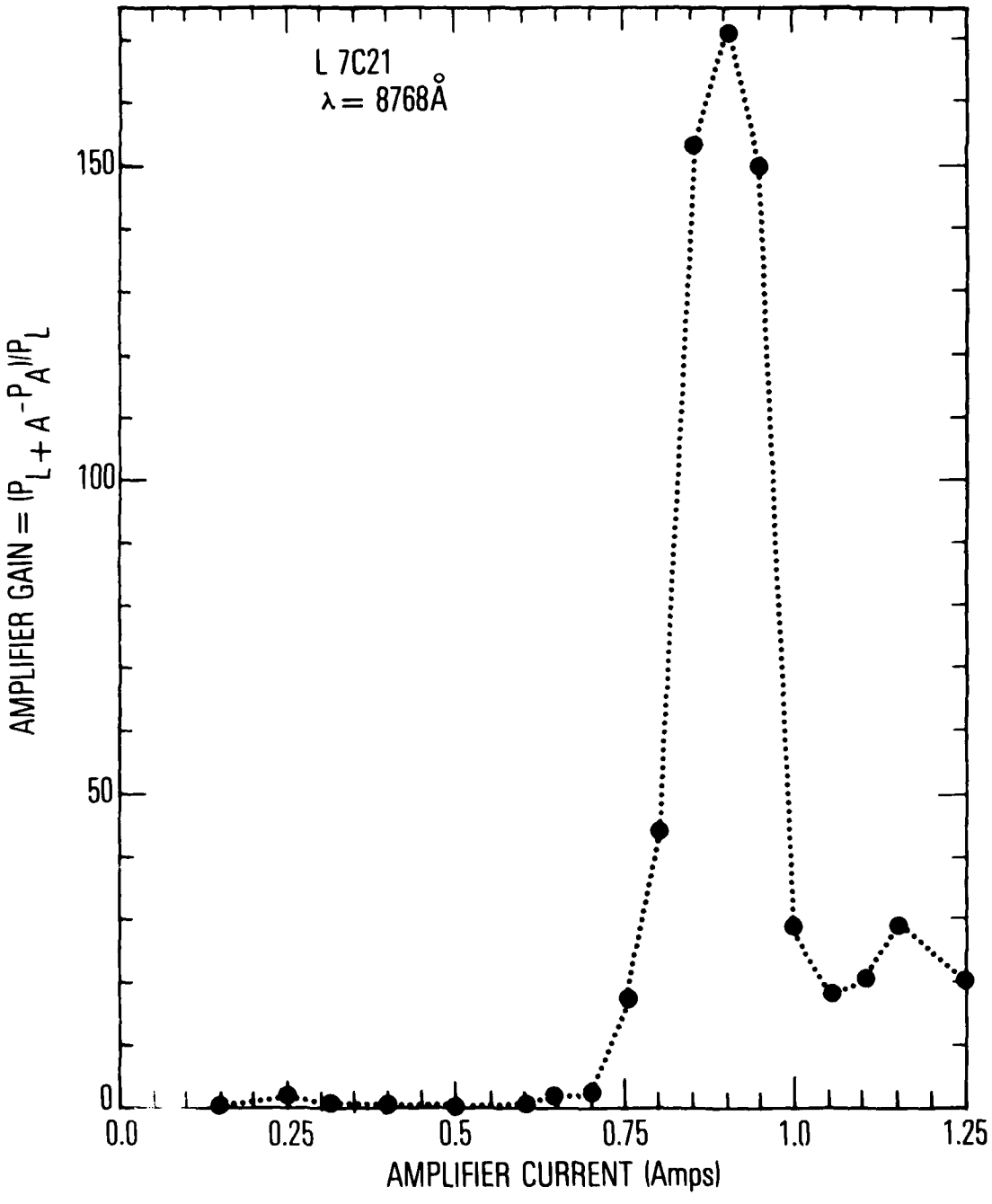

Fig. 7 True amplifier gain, as in Fig. 6, for the strong signal case at 8768Å.

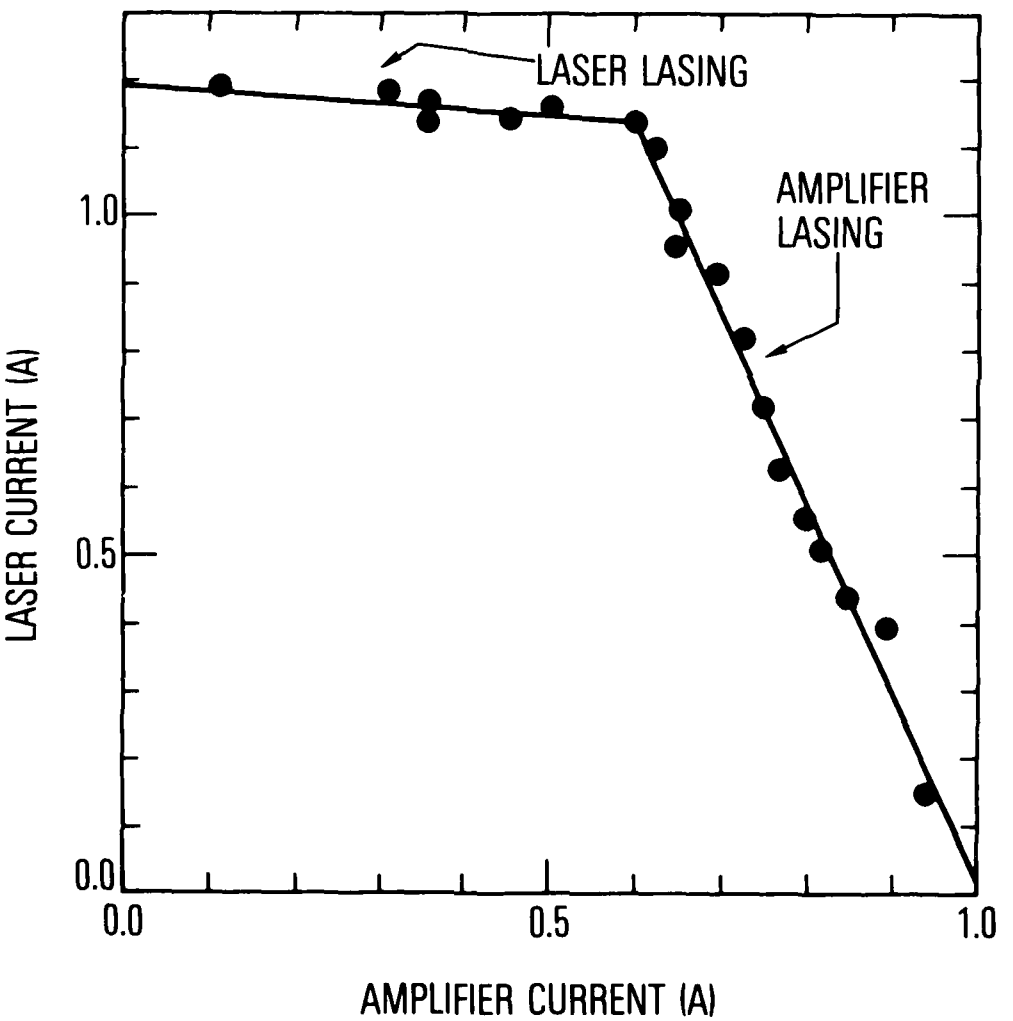

Fig. 8 Measurement of cracked substrate device threshold as a function of both the current to the laser portion and current to the amplifier portion.

threshold. If there were no interaction between the laser and amplifier, the threshold current should be constant. If the laser-amplifier acted as a single laser, however,the curve should be a straight line. The experimental curve shows that the light from a neighboring oscillator causes an effective lowering of the threshold. This phenomenon will be investigated more closely in the future.

Self-amplification

The possibility of using a laser below threshold as a regenerative amplifier is attractive for applications in optical communications and integrated optical circuits. Most of the previous work was done with homostructure lasers, [1] with the exception of Schicketanz and Zeidler.[2] Because of the multimode spectrum of many typical lasers and the difficulty of obtaining a frequency match between two individual lasers, we looked at laser amplification of its own light. In order to separate the amplified signal from the laser signal, we rotated polarization of the TE laser output before feeding it back into the active region, creating a TM polarized amplified signal. This allows a measurement of not only gains but also spatial variations of the gain. This method provides a more sensitive technique in measuring gain profiles than other techniques which look directly at the spontaneous emission.

The experimental set-up is shown in Fig. 9. Light emitted from face A of the diode is collimated, reflected off a mirror and refocused into the gain region at face A. This signal is amplified in the laser, emitted out face B, collected and focused onto the slit of a monochromator, and monitored by the photomultiplier tube (PMT). Two lenses instead of one are used in the feedback system to facilitate the positioning of the feedback signal. To focus the feedback signal back into the diode, the feedback mirror is placed at the image plane of the lens B. To distinguish the amplified light from the unamplified forward traveling light, a Fresnel rhomb was inserted into the feedback

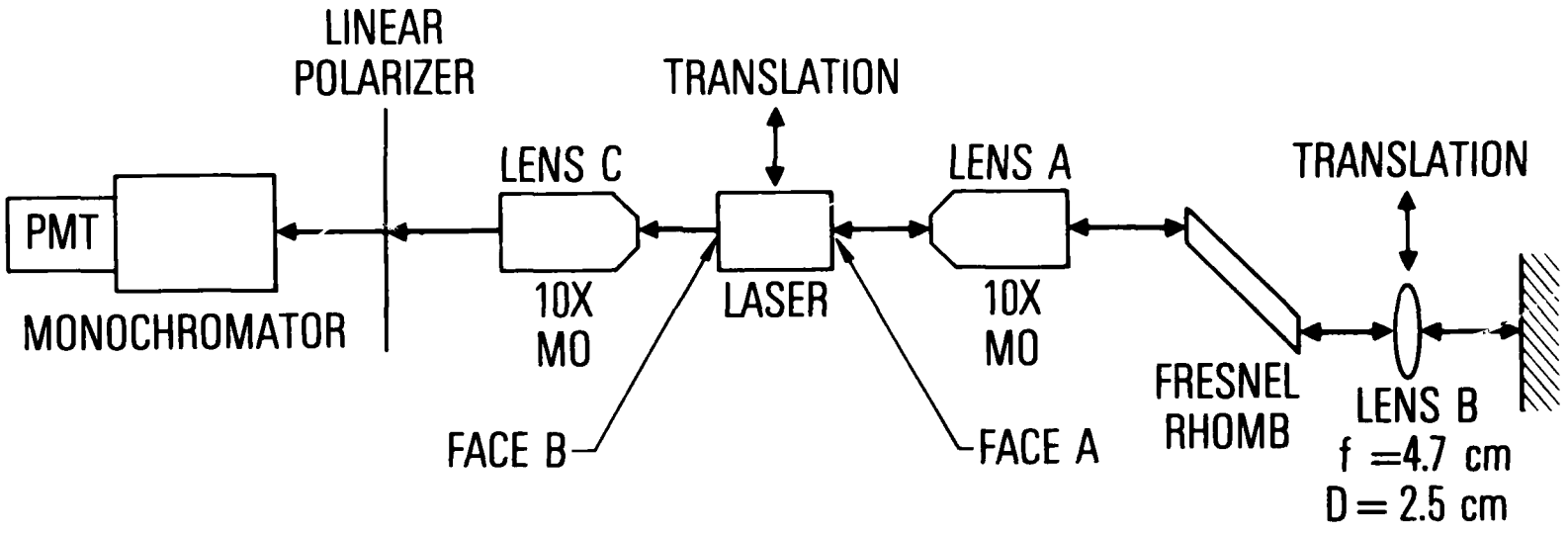

Fig. 9 Experimental setup for the study of self-amplification. TE polarized light exiting from face A is collimated through the Fresnel rhomb, retro-reflected off the mirror, returned through the rhomb and refocused into the laser diode as TM light. The signal is monitored at face B with a monochromator, allowing for the measurement of both polarizations.

system at the image plane of the microscope objective to rotate the feedback polarization by 90^{o}. Since the laser lases with a TE polarization, the double pass through the Fresnel rhomb results in amplified light with a TM polarization. A linear polarizer differentiated the amplified TM signal from the forward traveling TE signal. A monochromator (1/4m Jarrell-Ash) was used in a wide-band mode to filter out the fluorescence from the signal. A 50 μm entrance slit was used to provide spatial resolution, while no exit slit was used, resulting in a resolution of 200 $\overset{o}{A}$. The monochromator was tuned to the lasing wavelength.

The laser-amplifier was a DH GaAs diode with an active layer whose estimated thickness was about 0.2 μm. The laser was pulsed with a 100 ns pulse at a 100 HZ. The laser had a broad area contact (as opposed to a striped contact), although it had only a single lasing filament at the currents used. The total FWHM linewidth of the laser was 12 $\overset{o}{A}$ at 1.06 J_t. Due to line broadening, the individual longitudinal modes could not be resolved by the monochromator when narrower slits were used (the resolution was 0.8 $\overset{o}{A}$).

Two sets of measurements were made; the first being a scan of the TM gain profile, and the second being the amplified signal as a function of current. The gain profile was measured by translating the laser diode so as to direct the feedback signal into different regions of the P-N junction. The position of the amplified signal was maintained by appropriately translating the lens so that the signal could always be monitored by the PMT.

At the position of maximum gain, the current was varied to measure the amplification as a function of current. Because the laser output as well as the amplification varied with current, the TE forward travelling laser pulse was measured and used to normalize the amplified TM pulse. To separate the light coming directly off the front of the diode from the amplified light, both the TE and TM signals were

monitored with the feedback signal blocked and not blocked. By taking the appropriate sums and differences, the light from the front face and back face can be determined.

Gain Profile

A gain profile can be made directly by observing the spontaneous emission from the laser diode with a scanning detector. However, for weak gains, the signal is often obscured by the background noise. By using a probe beam and looking for amplification or attenuation, a more sensitive method is obtained for profiling diodes. Gain profiles are shown in Fig. 10 for different currents. The region over which gain is observed is broad, about 200 μm wide, and is offset in position from the lasing filament. Fig. 11 shows the position of the gain relative to the lasing filament. The vertical scale of the amplified signal is different from the vertical scale of the lasing filament so that no comparisons should be made of their relative strengths. There are two points of interest in Fig. 11. First, the maximum gain is not in the lasing filament but in a region corresponding to weak unpolarized spontaneous emission. Second, no gain is observed in the lasing filament.

The region of gain corresponds to a region of current injection below the threshold current. This region of current injection can be determined directly by observing the region of spontaneous emission. Fig. 11 shows the unpolarized spontaneous emission barely discernible above the background noise. A more sensitive technique is to probe the region of interest with a weak signal and look for amplification. In contrast to the weak direct signal is the amplified signal which clearly stands out above the noise. Because the amplified signal is dependent upon the current, this method provides a sensitive means to profile the current distribution. And, in turn, the nonuniformity of the wafer structure can be determined from the current distribution.

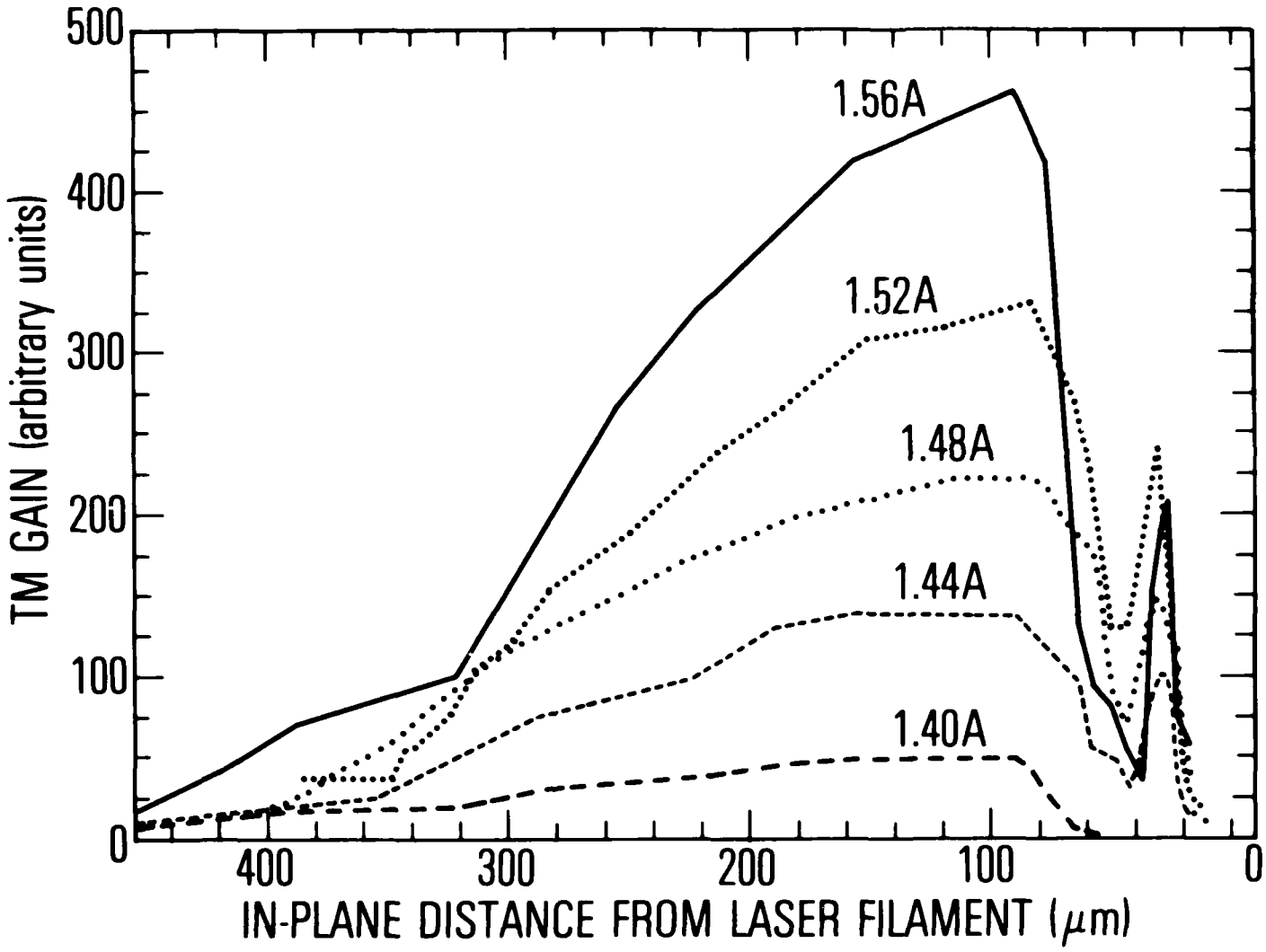

Fig. 10 Amplified signal (TM polarization) as a function of position in the junction plane. Zero is defined as the position of the TE laser filament. Measurements are made at several current levels.

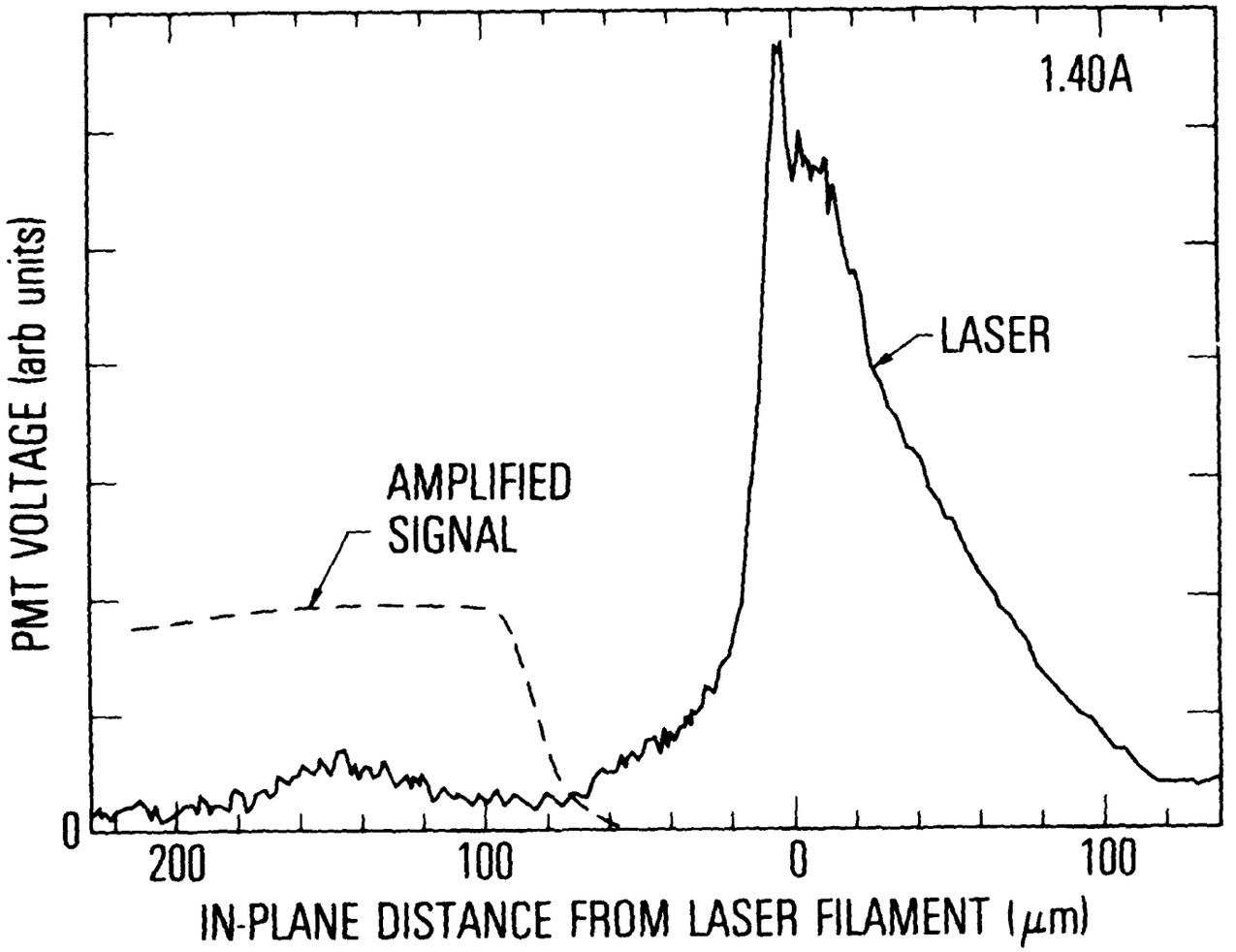

Fig. 11 Comparison of the position of the laser filament and the amplified signal in the plane of the diode junction.

An irregularity about 100 μm from the lasing filament is seen in the gain profile of Fig. 10 for currents greater than 1.48 amps. There are several possible explanations for this irregularity: 1) there may be an irregularity at the cleave surface, resulting in a lower transmission of the feedback signal, or 2) a bulk irregularity creating a local hotspot of current injection. The first reason could be caused by a bad cleave or a speck of dirt on the cleaved facet. However, this would result in a profile shape that is independent of the injected current. Since the irregularity is not seen for currents less than 1.44A and has a signal about half that of the maxmimum signal for currents greater than 1.44A, the first reason is not plausible. The second reason, a bulk irregularity, is a more probable cause. Due to irregularities in the bulk, local heating occurs which changes the current distribution. As the injected current is increased, the local heating effect is enhanced. This would result in a region of enhanced gain.

The lack of TM gain in the lasing filament can be explained by the TE polarization preference of the laser. Gain depends upon the absorption and re-emission of the input signal. Because absorption and emission are polarization dependent, only those carriers interacting with a photon whose polarization is the same as the input signal will contribute to the gain. Since the indigenous TE laser signal is much stronger than the injected TM signal and the number of carriers is finite, most of the carriers provide gain for the laser (TE). The remaining carriers provide gain for the injected TM signal but are not sufficient in number to produce a noticeable gain. If a noticeable gain for the TM signal were observed, a subsequent quenching of the laser signal would be observed. No quenching of the TE laser signal was observed when the TM signal was injected. Thus, in the case observed, the TE mode was dominant in the competition for carriers. Outside the lasing filament, this TE mode bias does not exist. The indigenous light outside the lasing filament is due to spontaneous emission and is not polarized. Hence, an input signal of any polarization can be amplified.

Gain Measurements

The unamplified laser signal from face B is the TE signal with the feedback blocked, TEB, while the amplified signal from face B is the difference between the TM signal with feedback and with the feedback blocked, TM-TMB. Both the unamplified laser signal and the amplified laser signal are shown in Fig. 12 as a function of the driving current. Because the input signal to the amplifier is proportional to the unamplified laser signal, the ratio between the amplified laser signal and the unamplified laser signal is proportional to the gain of the amplifier,

$$G = \xi \frac{TM - TMB}{TEB} \tag{37}$$

where

ξ = proportionality constant

= coupling efficiency .

The proportionality constant, ξ , is a result of losses in the feedback system. The relative gain, G/ξ , is shown in Fig. 13.

WEAK SIGNAL

The gain curve in Fig. 13 can be modelled by a weak signal regenerative amplifier for currents less than 1.52A. In this case, the gain curve is essentially exponential until the lasing threshold current is approached. As the threshold is approached, the gain curve deviates from that of an exponential and the curve becomes steeper. From the theory of regenerative amplifiers[3] and saturable amplifiers,[4] the weak signal gain equation is

$$\frac{I}{I_o} = \xi \frac{T^2 \exp(-a_o L) \exp(a_o L \eta h \nu J/P_S e)}{1 - R^2 \exp(2 a_o L \eta h \nu J/P_S e)} \tag{38}$$

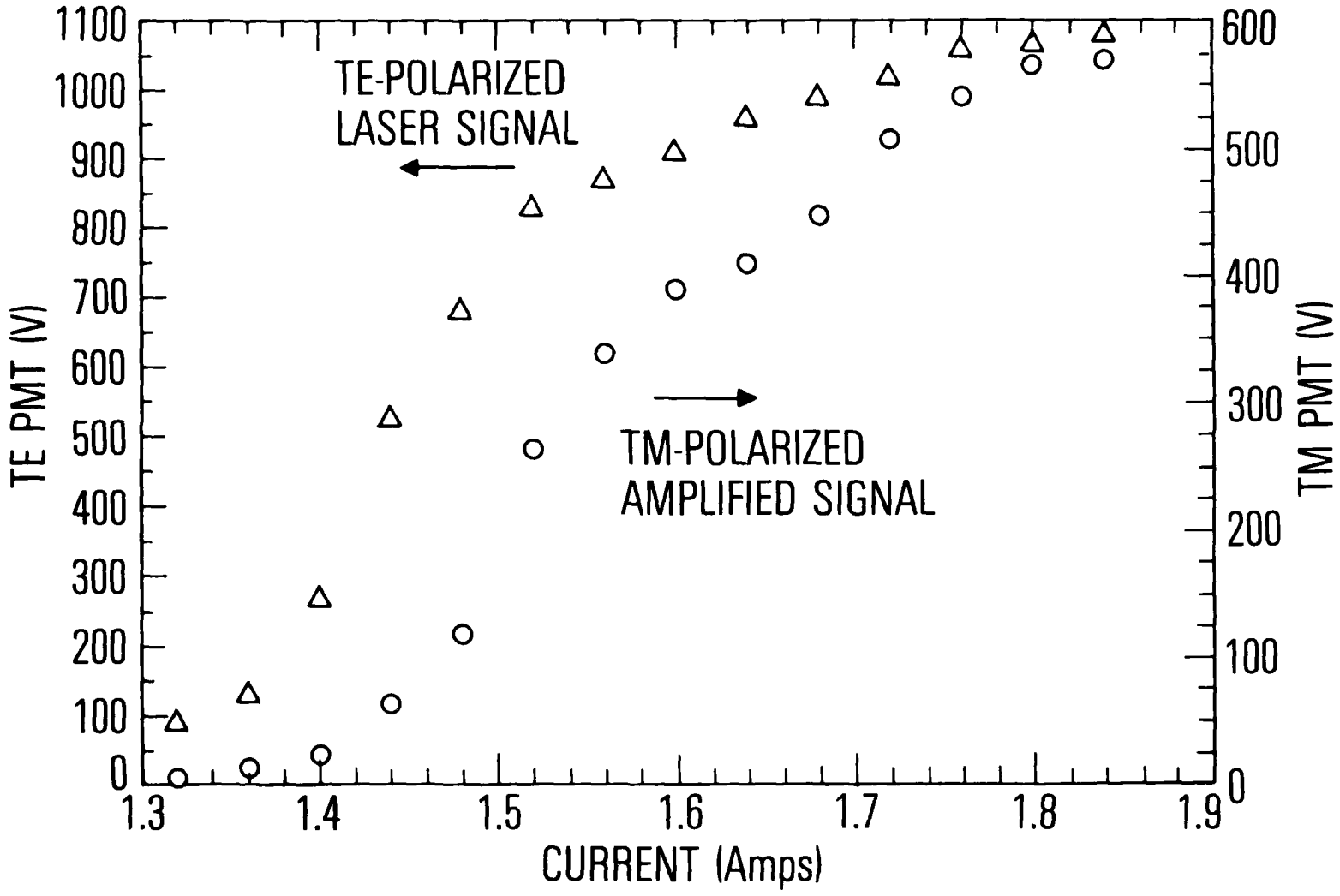

Fig. 12 Measurements of TM and TE polarized signal as a function of device current at the position of maximum gain in the junction plane.

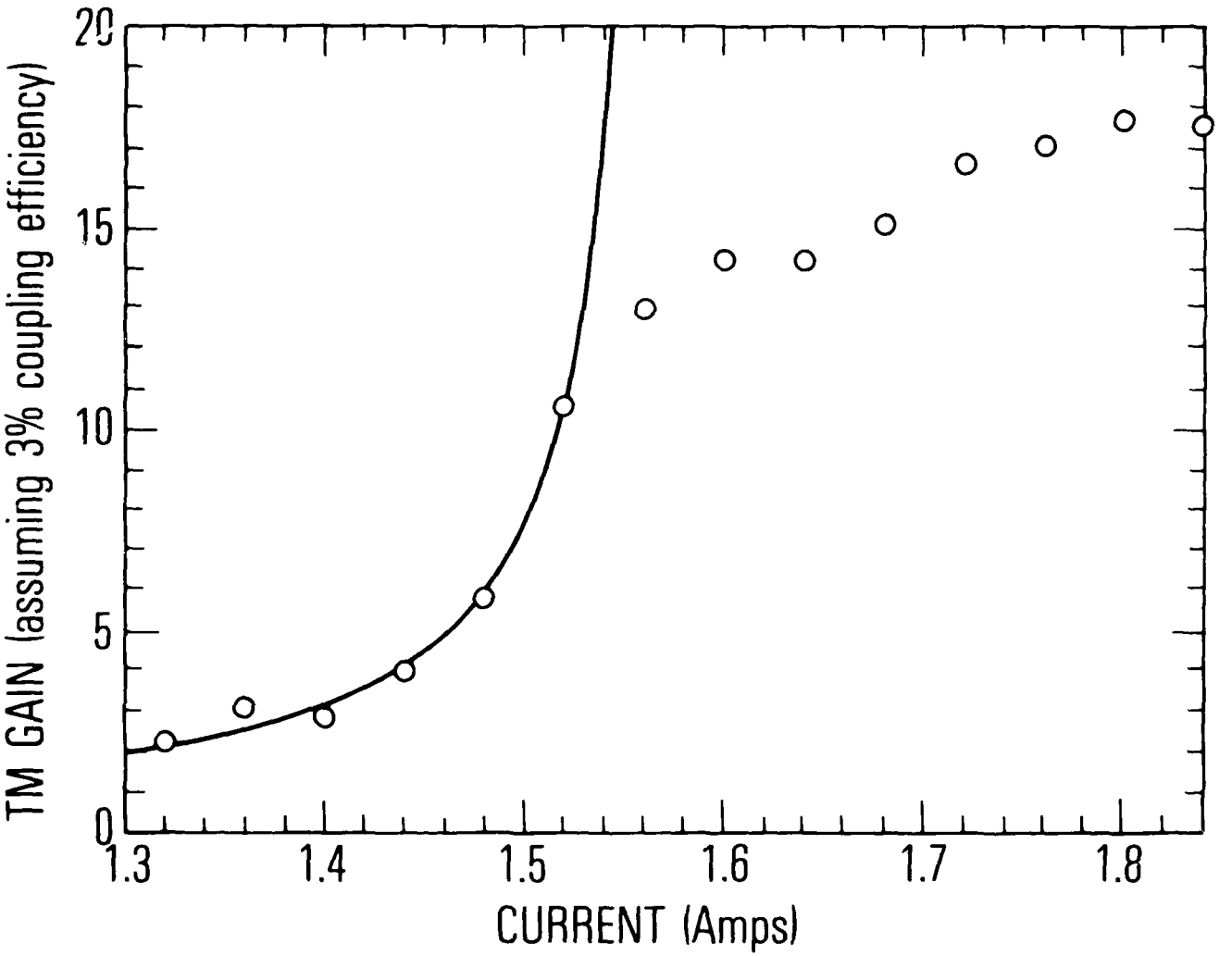

Fig. 13 Measurement of TM gain as a function of diode current. Theoretical curve for a regenerative amplifier is super-imposed onto the experimental results.

where

J = current to laser

ξ = coupling efficiency

a_o = small signal loss coefficient

L = Cavity length = 0.044 cm

η = internal quantum efficiency

$h\nu$ = photon energy

e = electronic charge

P_S = saturation power of the amplifier = $J_S\, dW$

d = active layer thickness

W = width of the lasing filament

Eq. (38) assumes that the individual modes of the amplifier cannot be distinguished (as is the case) so that the gain is average over the amplifier modes. A fit of the data to Eq. (38) yields a coupling efficiency of = 3.4% and a small signal loss coefficient of a = 26 cm^{-1}. This loss coefficient, a, is comparable to other values published in the literature.[95] The coupling efficiency was calculated to be less than 5%, taking into account the diffraction of the laser beam, the numerical apertures of the optics involved, and the error in focussing the lens. Experimental errors error can easily acount for the difference between the calculated value and the experimental value. From the relative gain curve in Fig. 13 and the experimental coupling efficiency of 3.4%, a gain as high as 15 is obtained for a laser signal.

The saturation power is the power of the lasing filament at which the weak signal and strong signal gain models are not longer valid. For powers much less than the saturation power, the weak signal model is valid, while for powers much greater than the saturation power, the strong signal model is valid. The saturation power can be obtained

from the coefficient of the exponential in Eq. (38) involving the current, $\frac{a_o Lh\nu\eta}{P_{Se}}$, provided that the current is known. However, the current in the amplifying region is not known; only the total injected current is known, so that the saturation power cannot be calculated. However, an upper limit for the saturation power can be made. Assuming that most of the injected current goes to the lasing filament and that the quantum efficiencies of the lasing filament and amplifier are equal, an estimate for the amplifier current can be made by noting the current at which the output of the lasing filament equals the output of the amplifier for a second current with the feedback blocked. The ratio of these currents is the efficiency in which current is injected into the amplifying region. It was found that this efficiency is less than 5%, resulting in an upper limit for the saturation power of 30 mW. This saturation power is greater than the power of the amplified beam, being consistent with small signal approximation.

REFERENCES

1. Coupland, et. al, Phys. Lett. 7 (4), 231 (Dec. 1963)

   "Measurement of Amplification in a GaAs Injection Laser"

   Crowe and Craig, APL 4 (3), 57 (Feb. 1969).

   "Small-Signal Amplification of GaAs Lasers"

   Crowe and Ahearn, IEEE - JQE, QE2 (8), 283 (Aug. 1966)

   "Semiconductor Laser Amplifier"

   Kosonocky and Cornely, IEEE - JQE, QE-4 (4), 125 (Apr. 1968).

   "GaAs Amplifiers"

2. Schicketanz and Zeidler, IEEE - JQE, QE-11 (2), 65 (Feb. 1975).

   "GaAs - Double-Heterostructure Lasers as Optical Amplifiers"

3. Ross, Lasers Light Amplifiers and Oscillators, Academic Press, NY 1969.

4. Stern, Proc. Physics of Quantum Electronics Conf., NY, McGraw-Hill 1966, "Saturation in Semiconductor Absorbers and Amplifiers of Light."

5. Kressel and Butler, Semiconductor Lasers and Heterojunction LEDs Academic Press, NY 1977, p. 263.

Appendix 1

The internal quantum efficiency, η, was experimentally determined from spontaneous emission measurements. The internal quantum efficiency is defined as

$$\eta = 1 - J_{sp}/J, \tag{A1}$$

where J is the total current density and J_{sp} is the current density which produces spontaneous emission. The current density is related to the power emitted from the diode by

$$\left(\frac{J_{sp}}{J}\right)^n = \frac{P_{sp}}{P_o} \tag{A2}$$

where

P_o = the power at thresholds

P_{sp} = the power due to spontaneous emissions

n = a heuristic parameter between 1 and 2 (n = 1 for an ideal diode)

By plotting ln (P_{sp}/P_o) vs ln (J_{sp}/J), the parameter n can be determined from the slope. Figure A shows such a plot with n = 1.1. Using equation (A2), the current density resulting in spontaneous emission, J_{sp}, can be calculated. Finally, from equation (A1), the internal quantum efficiency was determined to be 52%.

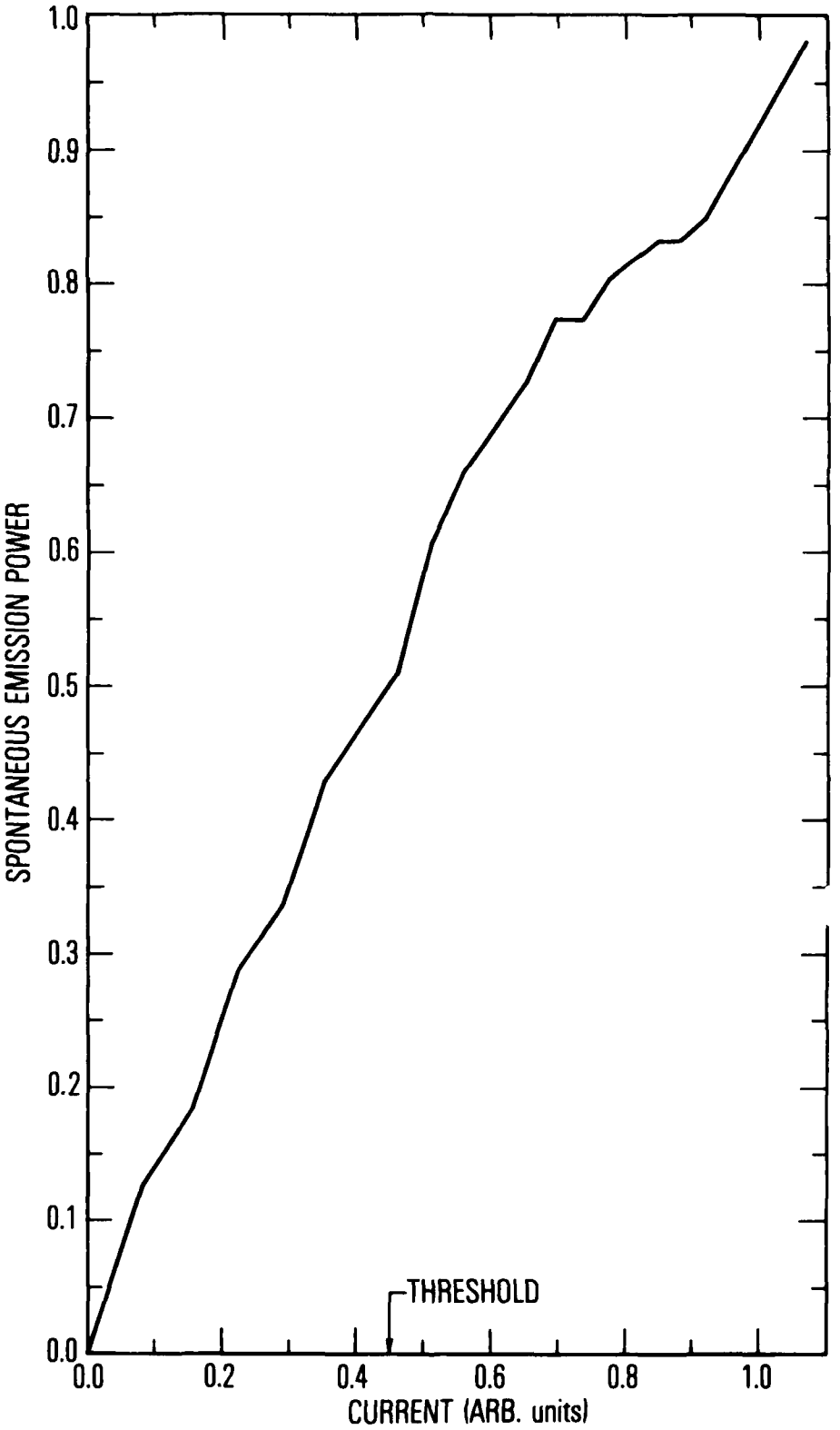

Fig. A Measurements of spontaneous emission power as a function of current. The slope of this function is used to determine the internal quantum efficiency.

LABORATORY OPERATIONS

The Laboratory Operations of The Aerospace Corporation is conducting experimental and theoretical investigations necessary for the evaluation and application of scientific advances to new military concepts and systems. Versatility and flexibility have been developed to a high degree by the laboratory personnel in dealing with the many problems encountered in the nation's rapidly developing space and missile systems. Expertise in the latest scientific developments is vital to the accomplishment of tasks related to these problems. The laboratories that contribute to this research are:

Aerophysics Laboratory: Launch and reentry aerodynamics, heat transfer, reentry physics, chemical kinetics, structural mechanics, flight dynamics, atmospheric pollution, and high-power gas lasers.

Chemistry and Physics Laboratory: Atmospheric reactions and atmospheric optics, chemical reactions in polluted atmospheres, chemical reactions of excited species in rocket plumes, chemical thermodynamics, plasma and laser-induced reactions, laser chemistry, propulsion chemistry, space vacuum and radiation effects on materials, lubrication and surface phenomena, photosensitive materials and sensors, high precision laser ranging, and the application of physics and chemistry to problems of law enforcement and biomedicine.

Electronics Research Laboratory: Electromagnetic theory, devices, and propagation phenomena, including plasma electromagnetics; quantum electronics, lasers, and electro-optics; communication sciences, applied electronics, semiconducting, superconducting, and crystal device physics, optical and acoustical imaging; atmospheric pollution; millimeter wave and far-infrared technology.

Materials Sciences Laboratory: Development of new materials; metal matrix composites and new forms of carbon; test and evaluation of graphite and ceramics in reentry; spacecraft materials and electronic components in nuclear weapons environment; application of fracture mechanics to stress corrosion and fatigue-induced fractures in structural metals.

Space Sciences Laboratory: Atmospheric and ionospheric physics, radiation from the atmosphere, density and composition of the atmosphere, aurorae and airglow; magnetospheric physics, cosmic rays, generation and propagation of plasma waves in the magnetosphere; solar physics, studies of solar magnetic fields; space astronomy, x-ray astronomy; the effects of nuclear explosions, magnetic storms, and solar activity on the earth's atmosphere, ionosphere, and magnetosphere; the effects of optical, electromagnetic, and particulate radiations in space on space systems.

THE AEROSPACE CORPORATION
El Segundo, California

• • •


DATE
FILMED
8